JSR Publications

Available Online

J. Sci. Res. **2** (3), 443-452 (2010)

JOURNAL OF SCIENTIFIC RESEARCH

www.banglajol.info/index.php/JSR

Improved Electrochemical Investigation of Combustion Synthesized Cd-doped $LiCoO_2$ Powders

S. Valanarasu[a], R. Chandramohan[b*] J. Thirumalai[b], and T. A. Vijayan[b]

[a]Physics Department, Ananda College, Devakottai-630303, India

[b]Physics Department, Sree Sevugan Annamalai College, Devakottai-630303, India

Received 12 February 2010, accepted in final revised form 9 August 2010

Abstract

The $LiCo_{1-x}Cd_xO_2$ (x = 0 to 0.1) cathode materials were synthesized by the combustion method (annealed at 800 °C for 12 h). Structural analyses of the synthesized materials were carried out using XRD. All the samples had the *R*-3*m* structure. $LiCo_{0.90}Cd_{0.1}O_2$ sample contained CdO phase as an impurity. Fourier transform infrared (FTIR) studies were carried out to understand the nature of the metal-ligand bond. The surface morphology and particle agglomeration was investigated using scanning electron microscope. The room temperature electrical conductivities of the sample increased with Cd content. For $LiCo_{1-x}Cd_xO_2$ (x = 0, 0.01, 0.03, 0.05 and 0.1), the first discharge capacity increased with increase in Cd content. Among these samples, $LiCo_{0.95}Cd_{0.05}O_2$ had good cycling performance (discharge capacity 195 mAh g^{-1} at n = 30).

Keywords: $LiCo_{1-x}Cd_xO_2$; Structural studies; Surface morphology; Conductivity; Discharge capacity.

DOI: 10.3329/jsr.v2i3.3877 J. Sci. Res. **2** (3), 443-452 (2010)

1. Introduction

Advances in electrode active material play a critical role on the development of lithium-ion batteries. Among the several cathode materials, lithium transition metal oxides have shown attractive electrochemical performance in the applications involving lithium battery devices and they are utilized as positive electrodes due to their high redox potential and specific capacity during the lithium intercalation/deintercalation processes [1]. $LiCoO_2$ is the most preferred cathode active material as it is widely used in commercial lithium-ion batteries and was first reported as cathode active material by Misushima et al. [2]. It is well known that the practical capacity of $LiCoO_2$ is limited to

* *Corresponding author*: chandru17@yahoo.com

around 140 $mAhg^{-1}$ i.e., nearly half of its theoretical capacity (273 $mAhg^{-1}$). This material has an ordered rock salt structure (α-$NaFeO_2$ structure) and belongs to R-3m space group. The high cost and toxicity of cobalt, however, makes the use of $LiCoO_2$ undesirable. In order to reduce the cost and to improve the cell voltage and specific capacity, attempts have been made to partially substitute cobalt with either transition metals or non-transition metals [3-5]. Recent attempts to improve the performance of $LiCoO_2$ by means of doping or coating have shown promising results for obtaining higher capacity with enhanced stability of the $LiCoO_2$ electrodes. Such modifications led to either improved capacity retention characteristics by suppressing the surface reactions of $LiCoO_2$ particles or higher achievable specific capacity by increasing the upper limit of the intercalation voltage through the formation of stronger M–O bonds and to stabilize the layered structure in its fully delithiated state [6]. Intensive investigations have been carried out on doped $LiCo_{1-y}M_yO_2$ oxides (M = Ti, Cr, Mn, Ni, Fe, Cu, Fe, Bi, Zn, Mo) [7-14], which show interesting structural and electrochemical properties. Doping with transition metals such as cadmium has gained increasing interest for the following reasons: (i) the low cost and low toxicity, (ii) the fact that cadmium substitution for transition metal oxides will increase the capacity, (iii) the cadmium doping stabilizes the layered structure and extends the cyclability and enhances the capability of the electrochemical cells. To the best of our knowledge, no study has been made on the Cd-doped $LiCoO_2$ cathode material so far. Thus, in the present work, we report on the synthesis of $LiCo_{1-x}Cd_xO_2$ powder by combustion technique. The influence of Cd on the material properties are discussed and correlated to the electrochemical properties of these cathode materials.

2. Experimental

For the synthesis of $LiCo_{1-x}Cd_xO_2$ (x = 0, 0.01, 0.03, 0.05 and 0.1) powders, a combustion route was adopted by the following procedure shown in Fig. 1. Calculated amount of 'water soluble' starch was dissolved in 20 ml of hot distilled water. To the hot starch solution was added stoichiometric amount of lithium hydroxide monohydrate ($LiOH.H_2O$), cobalt (II) nitrate hexahydrate ($Co(NO_3)_2.6H_2O$) and cadmium acetate $Cd(CH_3COO)_2 .2H_2O$ solutions that were (metal ions ratio Li:Cd:Co: is 1:x:1-x) mixed with starch solution. The obtained solution was evaporated at 80 °C for 6 hours with constant stirring. Continuous evaporation lead to the formation of a dark pink coloured polymeric resin. The polymeric resin was further dried at 120 °C for 12 hours to remove the excess water, which lead to the formation of a solid mass. Subsequently, these intermediates were heat treated at 800 °C for 12 hours. Unlike glycine, a molar correlation in terms of a chemical equation may not be possible in the case of starch. Being a polysaccharide $(–C_6H_{10}O_5–)_n$ starch does not have a definite *n* value [15].

The crystalline structure was determined by X-ray diffraction using X'pert PRO (PANalytical) diffractometer with CuKα radiation (λ = 0.15405 nm) and employing scanning rate of 5° min^{-1} over the 2θ range of 15-75 °. The particle size and morphology was examined using scanning electron microscope (SEM) Hitachi S-3000H model.

Infrared absorption spectra were recorded at room temperature using a Fourier transform interferometer (model Bruker IFS113v) in the range of 100-700 cm^{-1}. For SEM studies the samples are coated with Au using JFC-1100 model instrument. The electrical conductivity

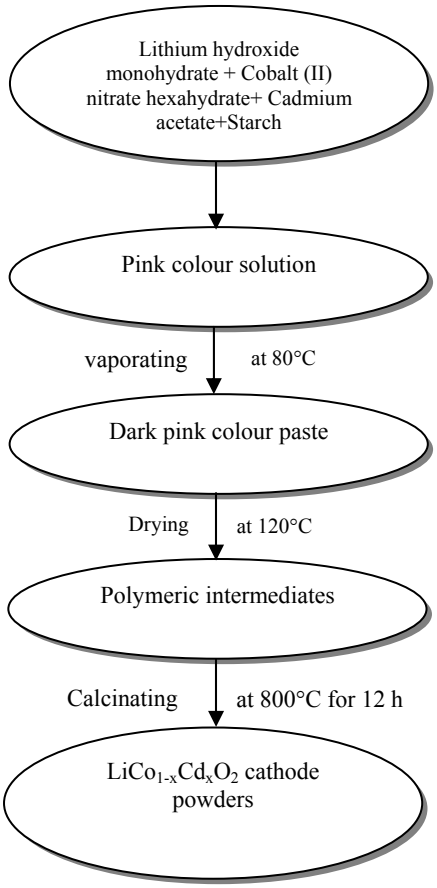

Fig. 1. Schematic of starch assisted combustion process for the synthesis $LiCo_{1-x}Cd_xO_2$ *(x* = 0, 0.01, 0.03, 0.05 and 0.1) cathode powders.

was measured by a two probe method from room temperature to 150 °C uniformly on circular pellets of diameter of ~10 mm and thickness of ~2 mm. The electrochemical performance was studied by assembling 2016 coin-type cells. Typical cathode was prepared from a slurry of the synthesized $LiCo_{1-x}Cd_xO_2$ powder (80 %), acetylene black (10 %) and (polyvinylidene fluride) PVDF binder (10 %) in n- methyl pyrrolidinone (NMP) solvent. The slurry was coated on an aluminium foil (current collector) and was dried at 110 °C in an oven for 12 hours. It was then pressed under a pressure of 4 tonne

inch^{-2}, for 1 min. Finally, circular discs of 18 mm diameter were cut and used as cathode. The cells were assembled using Li metal as anode and $LiPF_6$ in EC: DMC (1:1 vol.%) as electrolyte within an argon filled glove box. Galvanostatic discharge studies were carried out at a current rate of 0.1 C.

3. Results and Discussion

Fig. 2 shows the XRD patterns of $LiCo_{1-x}Cd_xO_2$ powders annealed at 800 ºC for 12 h. The presence of high intensity reflections are assignable to a highly crystalline and phase pure layered material and the peak signatures could be indexed to α-$NaFeO_2$ layered structure with R3m space group (JCPDS card no.: 75-0532). Further, the XRD pattern of $LiCo_{0.90}Cd_{0.1}O_2$ exhibits impurity peaks (marked with *) around diffraction angles 32.91º may be attributed to traces of CdO. It is apparent that such impurity peaks are not observed with $LiCo_{1-x}Cd_xO_2$ (x = 0, 0.01, 0.03, and 0.05) samples. The appearance of doublets at planes 0 0 6/1 0 2 and 1 0 8/1 1 0 indicate the stabilization of two-dimensional structure and an ordered distribution of lithium and cobalt ions in the inner lattice [16].

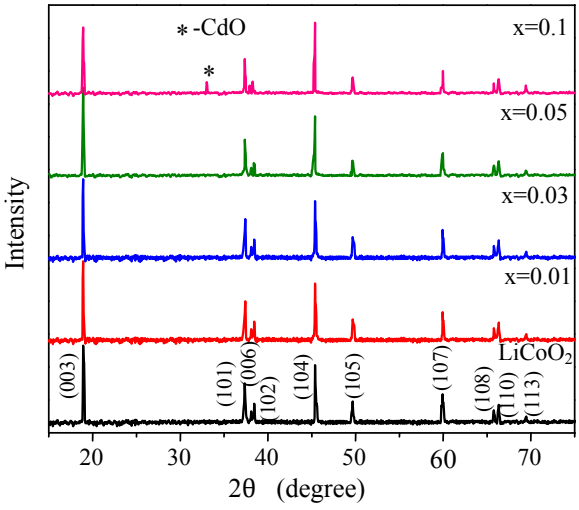

Fig. 2. X-ray diffraction patterns of $LiCo_{1-x}Cd_xO_2$ powders prepared by starch assisted combustion route method.

The lattice constants '*a*' and '*c*' were calculated for (003) and (104) planes using the formula given by

$$\frac{1}{d^2}=\left(\frac{4}{3}\right)\left[\frac{\left(h^2+hk+k^2\right)}{a^2}\right]+\left(\frac{l^2}{c^2}\right) \tag{10}$$

where (*h k l*) are the Miller indices of the plane concerned and *a* and *c* are the lattice constants are tabulated (Table 1). The lattice parameter *a* indicates the metal-metal intralayer distance while *c* represents the interlayer spacing [17]. Lattice substitution by elements with larger ionic radii often leads to expansion of the unit cell parameters. Thus, considering the large difference in ionic radii of Cd^{2+} (~0.103 nm) compared Co^{3+} (~ 0.063 nm), the observed increase in *a* and *c* values in $LiCo_{1-x}Cd_xO_2$ powders can be explained. These results indicates that addition of Cd stabilizes the layered structure of $LiCoO_2$ and increases the interlayer spacing with respect to that for pristine $LiCoO_2$ which would facilitate Li^+ ion intercalation-deintercalation. Further evidence of a good cation ordering is shown by a high *c/a* ratio value, which is greater than the critical value 4.899 (√24) [18] other than (x=0.1) sample. The intensity ratio value $I_{(0\,0\,3)}/I_{(1\,0\,4)}$ increases with increasing Cd molar concentration. However it decreases to 0.94 for $LiCo_{0.90}Cd_{0.1}O_2$ sample, less than the critical value of 1.2 [19], suggesting cation mixing at higher doping level.

Table 1. The lattice parameters of $LiCo_{1-x}Cd_xO_2$ samples.

x (Cd)	*d* (A˚)	*a* (A˚)	*c* (A˚)	*c/a*	$I_{(0\,0\,3)}/I_{(1\,0\,4)}$
0	4.670	2.836	14.011	4.94	1.29
0.01	4.675	2.851	14.026	4.92	1.33
0.03	4.680	2.854	14.041	4.92	1.38
0.05	4.687	2.864	14.062	4.91	1.41
0.1	4.692	2.897	14.077	4.86	0.94

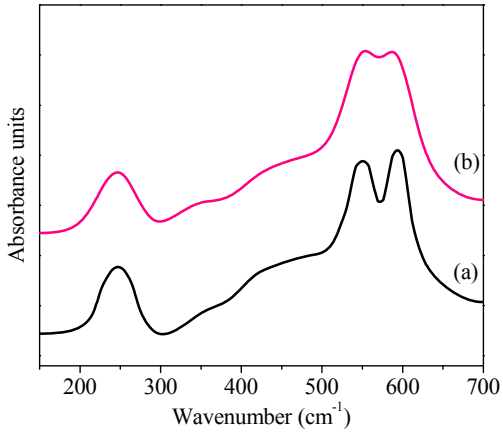

Fig. 3. FTIR spectra of a) $LiCoO_2$, b) $LiCo_{0.90}Cd_{0.1}O_2$ powders synthesized at 800°C.

FTIR features can be divided into two parts, the high wave-number region of strong absorption corresponding to the broad rock-salt band broken into several distinct components at ca. 600-400 cm^{-1}. An isolated strong band centered at ca. 240-250 cm^{-1} is observed (infrared active modes $2A_{2u}+2E_u$) in the low wave number region. Fig. 3 shows the FTIR spectra of $LiCoO_2$ and $LiCo_{0.90}Cd_{0.1}O_2$ samples. These results indicate the formation of compressed modes of CoO_6 and LiO_6 elongated octahedra. Upon Cd substitution, the vibrational mode of LiO_6 units is observed in the far-infrared region which remains quite stable. The shift has been observed toward the low-frequency side for solid solution with Cd (x=0.1) doping. These results show that, by doping, the local environment of lithium ions surrounded by oxygen anions is not affected and the CoO_2 layer covalency has increased slightly. Further, the broadening of the infrared peaks can be observed as an increase in CoO_6 distortion due to the addition of Cd in CoO_2 layers [20].

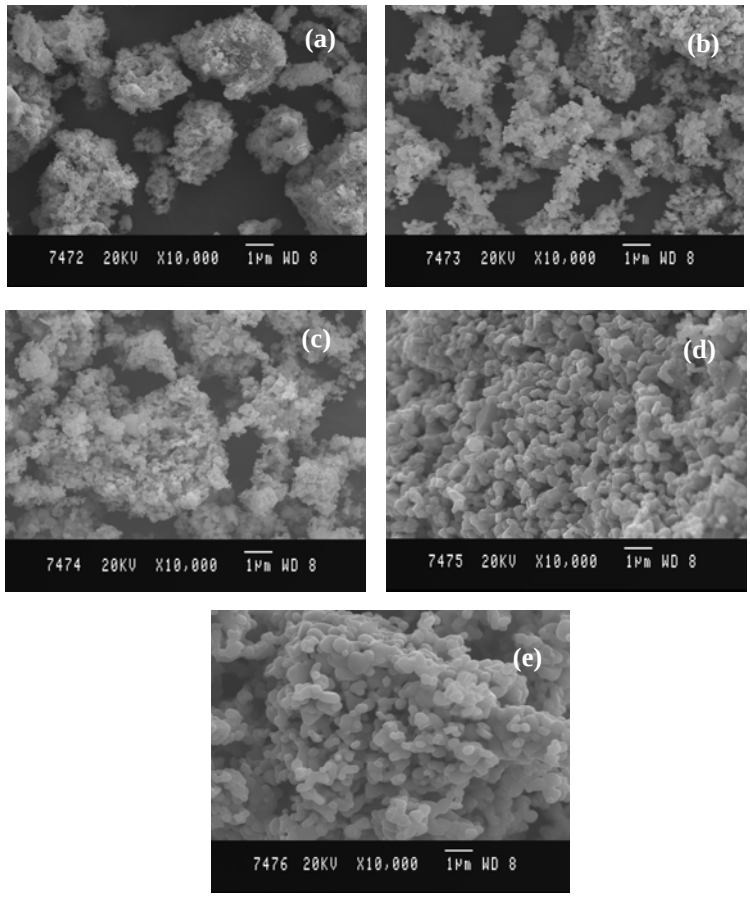

Fig. 4. SEM image of the $LiCo_{1-x}Cd_xO_2$ powders. (a) $LiCoO_2$, (b) $LiCo_{0.99}Cd_{0.01}O_2$, (c) $LiCo_{0.97}Cd_{0.03}O_2$, (d) $LiCo_{0.95}Cd_{0.05}O_2$, and (e) $LiCo_{0.90}Cd_{0.1}O_2$.

Fig. 4 shows the SEM photographs of $LiCo_{1-x}Cd_xO_2$ powders annealed at 800 ºC for 12 h. The particles are found to be well-defined facets that have a wide range of distribution ranging from 100 to 200 nm. The pristine $LiCoO_2$ sample contains bundle of agglomerated particles and relatively small particles on the agglomerates. Figs.4 (b) and (c) show agglomerated particles with less voids as compared to pristine sample. Uniformly distributed particles with good electrical contact between the particles were observed in Figs. 4 (d) and (e).

The electronic conductivity is a very important property of a cathode material. For a better charge transfer process during lithium intercalation-deintercalation in lithium-ion cell conductivity plays a significant role [21, 22]. Fig. 5 shows the electrical conductivity of $LiCo_{1-x}Cd_xO_2$ system measured from room temperature to 150 °C. The room temperature conductivity of pristine $LiCoO_2$ is found to be 4.52×10^{-5} Scm^{-1}. All the Cd-doped compounds show higher room temperature conductivity with respect to pristine $LiCoO_2$. The conductivity increases with increasing amount of Cd per mole of $LiCoO_2$. A conductivity value of 3.61×10^{-3} Scm^{-1} is observed for Cd (x=0.1) which is about two orders of magnitude higher than pristine $LiCoO_2$.

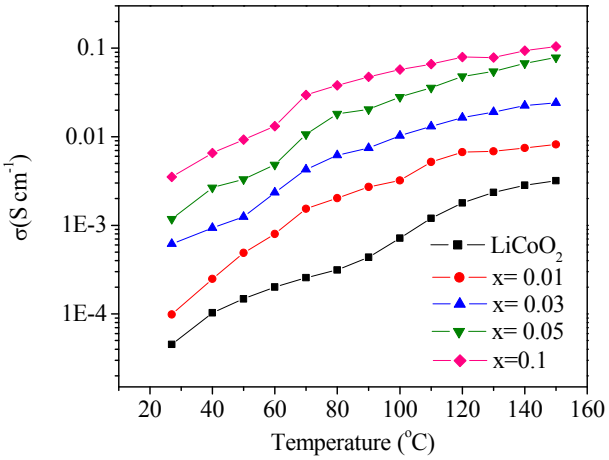

Fig. 5. Electrical conductivity profiles of $LiCo_{1-x}Cd_xO_2$ powders.

Electrochemical characterization was carried out by galvanostatic discharge cycling studies between 3.0 and 4.5 at the current density 0.1 mAg^{-1} employing 0.1 C rate. Fig. 6 shows the first discharge curves of $LiCo_{1-x}Cd_xO_2$ (x = 0, 0.01, 0.03, 0.05 and 0.1) powders. It is observed that Cd-doping increases the discharge capacity from 186 to 197mAg^{-1}. The first and 30th discharge capacities were measured for all the materials and thes are shown in Table 2. The increase of discharge capacity can be ascribed to the occupancy of Cd^{2+} ions in the inter-slab space along with Co^{3+} ions which facilitates the transit of Li^+ ions above 4.2 V. The relatively larger ionic radius of Cd^{2+} (~1.03 Å)

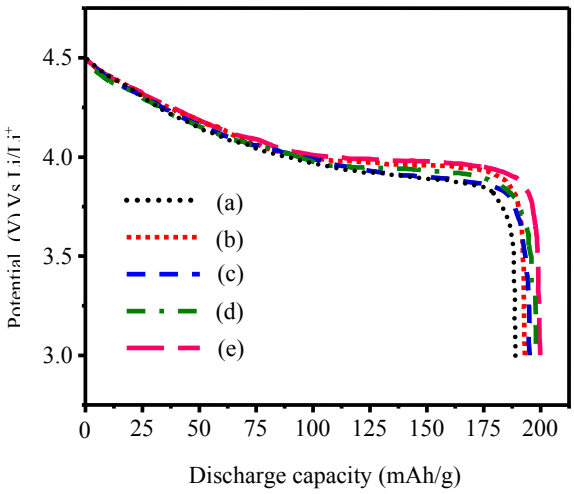

Fig. 6. Typical initial discharge capacity of the, $LiCo_{1-x}Cd_xO_2$ powders. (a) $LiCoO_2$, (b) $LiCo_{0.99}Cd_{0.01}O_2$, (c) $LiCo_{0.97}Cd_{0.03}O_2$, (d) $LiCo_{0.95}Cd_{0.05}O_2$, (e) $LiCo_{0.90}Cd_{0.1}O_2$.

Table 2. Cathode discharge and irreversible capacities of $LiCo_{1-x}Cd_xO_2$ sample.

Properties	Cd				
	x=0	x=.01	x=.03	x=.05	x=0.1
First discharge capacity (mAh g^{-1})	186	191	193	195	197
Reversible capacity in 30th cycle (mAh g^{-1})	155	171	175	185	175
Discharge capacity retention in 30th cycle (%)	83.3	89.5	90.7	94.9	88.8

than that of the Co^{3+} ion (0.63 Å) allow free movement of Li^+ ions due to pillaring effect [23,24] and also prevent the vacancy ordering. This fact is corroborated from the marginal increase observed in the '*c*' lattice (Table 1). As the charge-discharge proceeds the dopant ions located on the electrode surface form a solid solution with Co^{4+} ions. This solid solution acts as an intermediate layer and minimizes the dissolution of Co^{4+} ions into the electrolyte. This phase formation stabilizes the structure and enhances the cycle stability [23]. Nevertheless, the morphology and the uniformly distributed particles without voids of the Cd-doped $LiCoO_2$ also supplement the high discharge capacity as it obviously provides shorter diffusion path lengths for lithium-ion transport. Doping of Cd^{2+} in $LiCoO_2$ enhances the conductivity of $LiCoO_2$ as well as its structural stability as it creates more Co^{4+} ions due to charge compensation. Subsequently, Li^+ vacancies are generated to

balance the excess covalence greatly increase the conductivity of $LiCoO_2$ and thereby enhance the electrochemical performance [25]. The capacity fading rate f_c, is defined as

$$f_c = \frac{C_1 - C_n}{n} \quad (2)$$

where C_1 and C_n are the specific discharging capacities of first and *n*th cycle, and *n* is the number cycles. The capacity fading rate are 1.03, 0.66, 0.6, 0.33 and 0.73 $mAhg^{-1}$ per cycle for $LiCo_{1-x}Cd_xO_2$ (x = 0, 0.01, 0.03, 0.05 and 0.1) powders respectively. The capacity fading rate decreases first with increase in Cd content up to x=0.05 of Cd and then increases with Cd content x=0.1. $LiCo_{0.90}Cd_{0.1}O_2$ compound shows the decrease in reversible capacity due to cation mixing as revealed in XRD analysis The above results clearly show that the $LiCo_{0.95}Cd_{0.05}O_2$, show much better capacity retention in comparison to pristine $LiCoO_2$.

4. Conclusion

$LiCo_{1-x}Cd_xO_2$ has been successfully synthesized by starch assisted combustion route method. XRD patterns suggest that Cd-doping favours the formation of highly layered structure with marginally expanded '*c*' lattice thereby providing more space for lithium-ion intercalation/deintercalation. Microscopy studies reveal that the particle size increases with the increase of dopant content In addition, the doping enhances the conductivity thereby improving the reversibility of the electrode reaction. $LiCo_{0.95}Cd_{0.05}O_2$ deliver an average discharge capacity of around 195 $mAhg^{-1}$ suggesting that Cd-doping enhances the electrochemical performance of $LiCoO_2$.

Acknowledgement

The authors R. Chandramohan and S. Valanarasu thank the University Grants Commission (UGC-SERO), Hyderabad, India for the financial support for this work.

References

1. T. Ohzuku, A. Ueda, Solid-State Ionics **69**, 201(1994). doi:10.1016/0167-2738(94)90410-3
2. K. Misushima, P. C. Jones, P.J. Wiseman, J.B. Goodenough, Mater. Res. Bull. **15,** 783 (1980). doi:10.1016/0025-5408(80)90012-4
3. C. Delmas, I. Saadoune, A. Rougier, J. Power Sources **44,** 595(1993). doi:10.1016/0378-7753(93)80208-7
4. K. K. Lee, K. B. Kim, J. Electrochem. Soc. **147,** 1709 (2000). doi:10.1149/1.1393422
5. C. Delams, I. Saadoune, Solid-State Ionics **53,** 370 (1992). doi:10.1016/0167-2738(92)90402-B
6. Z. X.Wang, L. J. Liu, L. Q. Chen, and X. J. Huang, Solid-State Ionics **148,** 335 (2002). doi:10.1016/S0167-2738(02)00071-1
7. S. Gopukumar, Y. Jeong, K. B. Kim, Solid State Ionics **159,** 223 (2003).

doi:10.1016/S0167-2738(03)00081-X
8. C. D. Jones, E. Rossen, J. R. Dahn, Solid State Ionics **68,** 65 (1994). doi:10.1016/0167-2738(94)90235-6
9. C. Julien, M. A. Camacho-Lopez, T. Mohan, S. Chitra, P. Kalyani, S. Gopukumar, Solid State Ionics **135,** 241 (2000). doi:10.1016/S0167-2738(00)00370-2
10. I. Sadoune, C. Delmas, J. Solid State Chem. **136,** 8 (1998). doi:10.1006/jssc.1997.7599
11. H. Kobayashi, S. Shigemura, M. Tabuchi, H. Sakaebe, K. Ado, H. Kageyama, A. Hirano, R. Kanno, M. Wakita, S. Morimotoand Nasu, J. Electrochem. Soc. **147,** 960 (2000). doi:10.1149/1.1393298
12. M. Zou, M. Yoshio, S. Gopukumar, J. I. Yamaki, Chem. Mater. **15,** 4699 (2003). doi**:** doi:10.1021/cm0347032
13. M. Zou, M. Yoshio, S. Gopukumar, J. I.Yamaki, Chem. Mater. **17,** 1284 (2005). doi:10.1021/cm048734o
14. S.A. Needham, G. X. Wang, H. K. Liu, V. A. Drozd, and R. S. Liu, J. Power Sources **174,** 828 (2007). doi:10.1016/j.jpowsour.2007.06.228
15. P. Kalyani, N. Kalaiselvi, N. Muniyandi, Mater. Chem. Phys. **77,** 662 (2002). doi:10.1016/S0254-0584(02)00132-3
16. H. Y. Xu, S. Xie, C. P. Zhang, C. H. Chen, J. Power Sources, **148,** 90 (2005). doi:10.1016/j.jpowsour.2005.02.005
17. P. Kalyani, N. Kalaiselvi, N. Muniyndi, J. Power Sources, **111,** 232 (2002). doi:10.1016/S0378-7753(02)00307-5
18. S. Madhavi, G.V. Subba Rao, B.V.R Chowdari, S. F. Y. Li, J. Electrochem. Soc. **148,** A1279 (2001). doi:10.1149/1.1410968
19. T. Lee, K. Cho, J. Oh, D. Shin, J. Power Sources **174,** 394 (2007). doi:10.1016/j.jpowsour.2007.06.136
20. C. Julien, Solid State Ionics **157,** 57 (2003). doi:10.1016/S0167-2738(02)00190-X
21. S. Huang, Z. Wen, X. Yang, Z. Gu, X. Xu, J. Power Sources **148,** 72 (2005). doi:10.1016/j.jpowsour.2005.02.002
22. P. Ghosh, S. Mahanty, and R.N. Basu, Mater. Chem. Phys. **110,** 406 (2008). doi:10.1016/j.matchemphys.2008.02.030
23. H. S. Kim, T. K. Ko, B. K. Na, W. I. Cho, and B. W. Chao, J. Power Sources **138,** 232 (2004). doi:10.1016/j.jpowsour.2004.06.024
24. T. Ohzuku and A. Ueda, J. Electrochem. Soc. **141,** 2972 (1994). doi:10.1149/1.2059267
25. F. Nobili, F. Croce, B. Scrosati, and R. Marassi, Chem. Mater. 13, 1642 (2001). doi:10.1021/cm000600x